A quantum critical point at the heart of high temperature superconductivity

B. J. Ramshaw,[1] S. E. Sebastian,[2] R. D. McDonald,[1] James Day,[3] B. Tan,[2] Z. Zhu,[1]
J.B. Betts,[1] Ruixing Liang,[3,4] D. A. Bonn,[3,4] W. N. Hardy,[3,4] and N. Harrison[1]

[1]*Mail Stop E536, Los Alamos National Labs, Los Alamos, NM 87545**

[2]*Cavendish Laboratory, Cambridge University,*
JJ Thomson Avenue, Cambridge CB3 OHE, U.K

[3]*Department of Physics and Astronomy,*
University of British Columbia, Vancouver V6T 1Z4, Canada

[4]*Canadian Institute for Advanced Research, Toronto M5G 1Z8, Canada*

(Dated: April 27, 2014)

In the quest for superconductors with high transition temperatures (T_c s), one emerging motif is that unconventional superconductivity is enhanced by fluctuations of a broken-symmetry phase near a quantum-critical point. While recent experiments have suggested the existence of the requisite broken symmetry phase in the high-T_c cuprates, the signature of quantum-critical fluctuations in the electronic structure has thus far remained elusive, leaving their importance for high-T_c superconductivity in question. We use magnetic fields exceeding 90 tesla to access the underlying metallic state of the cuprate $YBa_2Cu_3O_{6+\delta}$ over an unprecedented range of doping, and magnetic quantum oscillations reveal a strong enhancement in the quasiparticle effective mass toward optimal doping. This mass enhancement is a characteristic signature of quantum criticality, and identifies a quantum-critical point at $p_{crit} \approx 0.18$. This point also represents the juncture of the vanishing pseudogap energy scale and the disappearance of Kerr rotation, the negative Hall coefficient, and the recently observed charge order, suggesting a mechanism of high-T_c that is strongest when these definitive experimental signatures of the underdoped cuprates converge at a quantum critical point.

In several classes of unconventional superconductors, such as the heavy fermions, organics, and iron pnictides, the growing consensus is that superconductivity is linked to a quantum critical point, where these systems undergo a phase transition at zero temperature, and quantum fluctuations enhance the interactions that give rise to superconductivity (1, 2). These fluctuations produce strong electronic correlations approaching the quantum critical point (QCP), resulting in an experimentally-observable enhancement of the electron effective mass (1, 3–6). It is widely believed that spin fluctuations in the vicinity of an antiferromagnetic QCP are important for superconductivity in many heavy-fermion, organic, and pnictide superconductors(2, 7), leading to the ubiquitous phenomenon of a superconducting dome surrounding a QCP. The role of quantum-criticality in cuprate high-temperature superconductors is more controversial (8): do the collapsing experimental energy scales(9), enhanced superconducting properties(9, 10), and evidence for a change in ground-state symmetry near optimal doping(11–15) indicate an associated QCP with strong fluctuations that are relevant to superconductivity(2, 16–18)? Alternative explanations for the phenomenol-

* Corresponding author: bradramshaw@gmail.com

ogy of the cuprate phase diagram focus on the physics of a lightly doped Mott insulator (8, 19), rather than a metal with competing phases and a QCP. Establishing whether there is a QCP near optimal doping is therefore crucial to find the right starting point for a theory of high-T_c. Several investigations, both theoretical and experimental, suggest that competing order is present in the cuprates, and is associated with the charge (rather than spin) degree of freedom (such as charge density wave order, orbital current order, or nematicity, see Figure 1)(12, 14–17, 20–27). What has been missing until now is direct, low-temperature evidence that the change in ground-state symmetry near optimal doping is accompanied enhanced electronic correlations in the ground state that would unambiguously identify $p \approx 0.18$ as a QCP.

A powerful technique for measuring low-temperature Fermi surface properties is the magnetic quantum-oscillation phenomenon, which directly accesses quasiparticle interactions through the effective mass(28). While such measurements have been successful in identifying QCPs in lower-T_c materials (e.g., $CeRhIn_5$ and $Ba(FeAs_xP_{1-x})_2$ (3, 5)), the robustness of superconductivity near optimal doping in the cuprates has impeded these measurements, and ground-state signatures of a QCP, such as an enhanced effective mass, have remained elusive. The Fermi surface in underdoped cuprates is known to be relatively small and electron-like(29–33) in contrast to overdoped cuprates where a much larger hole-like surface is observed (34). This suggests the existence of broken translational symmetry in the underdoped cuprates that "reconstructs" the large hole-like surface into the smaller electron-like surface: this translational symmetry breaking is likely related to the charge order observed in the same doping range as the small Fermi pockets(14, 26). This makes a systematic study of the doping dependence of these small pockets as they approach optimal doping imperative, and in a single compound so that trends with doping are unambiguous. We use high magnetic fields, extending to over 90 T, to suppress superconductivity and access quantum oscillations of the underlying Fermi surface over nearly twice the range of dopings than previously possible in a single compound (orange stars in Figure 1.) We report the first observation of quantum oscillations in $YBa_2Cu_3O_{6+\delta}$ at $\delta = 0.75$, 0.80, and 0.86 (nominal hole doping $p = 0.135, 0.140,$ and 0.152), shown in Figure 2a. $YBa_2Cu_3O_{6.86}$, with a T_c of 91 ± 1 K, brings our Fermi-surface measurements close to optimal doping ($T_c \approx 94$K) where superconductivity is most robust both in temperature and magnetic field(10). We observe a continuous evolution of the small Fermi surface pocket area (Figure 2b), while the temper-

ature dependence of the quantum oscillations reveals a strong enhancement of the effective mass with increased hole doping (Figure 3). The weak change in Fermi surface area suggests that the observed mass enhancement is not the result of evolving band structure, but is instead a reflection of enhanced electronic interactions due to fluctuations in the vicinity of a QCP.

The magnetoresistance of $YBa_2Cu_3O_{6.86}$, $YBa_2Cu_3O_{6.80}$, and $YBa_2Cu_3O_{6.75}$ is shown in the left panels of Figure 2a. Three regimes are clearly seen in the data: zero resistance up to the vortex melting field; increasing resistance in the vortex-liquid regime; and, magnetoresistance accompanied by oscillations in the normal state. We subtract a smooth and monotonic background from the magnetoresistance to obtain the oscillatory component (see S.I. for details of the background subtraction and the data analysis). Two trends with doping are immediately apparent: (1) at higher doping the oscillation amplitude grows faster with decreasing temperature; and (2), the oscillation frequency changes very little between $p = 0.135$ and $p = 0.152$. The first observation directly indicates an increasing effective mass; the second observation constrains the doping where the reconstruction from large to small Fermi surface takes place. We quantify these observations below.

The evolution of the quantum oscillation temperature dependence with doping, and how it relates to the effective mass, can be understood quantitatively within the Lifshitz-Kosevich formalism, which has been used successfully to analyse oscillations in cuprates at lower hole doping(22, 31–33, 35). Quantum oscillations are suppressed with increasing temperature via the ratio of thermal to cyclotron energy, $\frac{k_B T}{\hbar \omega_c^\star}$, where $\omega_c^\star \equiv \frac{eB}{m^\star}$ is the frequency at which a quasiparticle of effective mass $m^\star$, charge e, in a magnetic field B, completes a cyclotron orbit. We extract the oscillation amplitude at each temperature and fit it to the functional form of this thermal suppression(28) (see Methods),

$$A(T) = \frac{2\pi^2 \frac{k_B T}{\hbar \omega_c^\star}}{\sinh\left(2\pi^2 \frac{k_B T}{\hbar \omega_c^\star}\right)}, \tag{1}$$

yielding the effective mass $m^\star$ (see Figure 3a and Figure 3b). This effective mass is the fully-renormalized, thermodynamic cyclotron effective mass, which is enhanced over the bare "band mass" by interactions in the system(28). The effective mass is plotted as a function of doping in Figure 3c, which reveals an increase in the mass of almost a factor of three from $p = 0.116$ to $p = 0.152$, strongly suggesting mass enhancement due to increasing electronic interactions in the ground state of $YBa_2Cu_3O_{6+\delta}$ approaching a QCP near optimal doping.

Note that electron-phonon coupling is generally observed to *decrease* with increasing hole doping, ruling it out as the mechanism for mass enhancement (36).

The quantum oscillation frequency F gives the Fermi surface area through the Onsager relation(28), $A_k = \frac{2\pi e}{\hbar} F$, where A_k is the Fermi surface area in momentum space perpendicular to the magnetic field. In contrast to the effective mass, which is strongly enhanced, the Fermi surface area only evolves weakly toward optimal doping: Figure 2b shows F increasing by roughly 20% from $p \approx 0.09$ to $p \approx 0.152$. The observation of the small Fermi surface pocket up to $p \approx 0.152$ requires that the reconstruction of the Fermi surface also persists up to this doping, strongly suggesting that the reconstruction is related to the incommensurate charge order also observed in this doping range (14, 23, 25, 26). The large increase in effective mass, with no accompanying large change in Fermi surface area, suggests that the mass enhancement results from increasing electronic interactions in the proximity of a QCP (1, 37), and not from a simple chemical potential shift in a rigid band structure.

The connection between the mass enhancement we observe in quantum oscillations and high-T_c superconductivity is evident in Figure 4, which shows successive T_c curves in increasing magnetic field. By 30 T—the third-highest curve in Figure 4—superconductivity persists only in two small domes centred around $p \approx 0.08$ and $p \approx 0.18$; by 50 T only the region around $p = 0.18$ remains. This phase diagram of $YBa_2Cu_3O_{6+\delta}$ in high field, with T_c first suppressed to zero around $p \approx 0.125$, closely resembles that of $La_{2-x}Ba_xCuO_4$ in zero field, where static charge and stripe order are observed(38). To emphasize the enhancement of the effective mass, we plot $1/m^\star$ on this phase diagram (including previous $m^\star$ measurements at lower doping(39)). This shows a trend toward maximum mass enhancement at $p \approx 0.08$ and $p \approx 0.18$—the same dopings at which superconductivity is the most robust to applied magnetic fields. This is consistent with the maxima observed in the upper critical field H_{c2} (10), which is enhanced by a large density of states (proportional to the mass). The jump in the specific heat at T_c, related to the condensation energy and also enhanced by a large effective mass, also shows a peak near $p \approx 0.18$ (9). This observation of maxima in several thermodynamic quantities is characteristic of a QCP, having been observed in many heavy fermion systems (37) and an iron pnictide (5) (see S.I for further discussion). One possible scenario is that critical fluctuations surrounding $p_{crit} \approx 0.08$ and $p_{crit} \approx 0.18$ provide two independent pairing mechanisms, analogous to the two superconducting domes in $CeCu_2Si_2$ that originate at antiferromagnetic and valence-transitions QCPs(40). A second scenario is

a single underlying pairing mechanism whose strength varies smoothly with doping(41), but which is enhanced at the critical points by an increased density of states as $m^\star$ increases, and/or by quantum-critical dynamics.

Given that our observed mass enhancement establishes $p_{crit} \approx 0.18$ as a QCP, it is natural to ask what the associated broken symmetry phase is. The hole doping $p_{crit} \approx 0.18$ represents the juncture of several doping-dependent phenomena associated with underdoped cuprates. First, $p \approx 0.19$ represents the collapse to zero of energy scales associated with the formation of the pseudogap which onsets at temperature $T^\star$ (9). Second, the onset of an anomalous polar Kerr rotation and neutron spin flip scattering both terminate at $p \approx 0.18$ (11, 12), representing an unidentified form of broken symmetry (that persists inside the superconducting phase for the Kerr experiment). Third, in high magnetic fields, both the sign-change of Hall coefficient, from positive to negative, and the onset of long-range order observed by NMR, go to zero near $p \approx 0.18$(23, 42), suggesting that Fermi surface reconstruction from electron-like to hole-like occurs at this doping. Finally, $p \approx 0.18$ represents the maximum extent of incommensurate charge density wave (CDW) order reported in several different experiments (14, 23, 26). While the Fermi surface reconstruction is likely related to this CDW order, its short correlation length and the weak doping dependence of its onset temperature appears to be at odds with the traditional picture of long range order collapsing to $T = 0$ at a QCP. Two scenarios explaining fity at $p_{crit} \approx 0.18$ immediately present themselves. In the first scenario, the suppression of superconductivity by an applied magnetic field allows the CDW to transition to long-range order, as suggested by X-ray, NMR, and pulsed-echo ultrasound experiments.(23, 25, 43) In this first instance, we would be observing a field-revealed QCP. In the second scenario, CDW order is co-existent with another form of order that also terminates at $p_{crit} \approx 0.18$. Such a coexistence is suggested by multiple experimental results, including but not limited to Nernst anisotropy(21) and the anomalous polar Kerr effect(11). In this second scenario, the CDW reconstructs the Fermi surface and the other hidden form of order drives the quantum-criticality. That $p \approx 0.18$ is a critical doping in zero magnetic field(9, 11, 15) suggests that the quantum-critical fluctuations—that enhance the effective mass—exist without an applied field. Regardless of the specific mechanism, the coincidence of the diverging effective mass with region of most robust superconductivity implies that

quantum-criticality is integral to high-T_c.

---

[1] P Coleman, C Pepin, QM Si, and R Ramazashvili. How do fermi liquids get heavy and die? *Journal of Physics-Condensed Matter*, 13(35):R723–R738, SEP 3 2001. ISSN 0953-8984. doi:10.1088/0953-8984/13/35/202.

[2] Louis Taillefer. Scattering and pairing in cuprate superconductors. In JS Langer, editor, *Annual Review of Condensed Matter Physics, Vol 1*, volume 1 of *Annual Review of Condensed Matter Physics*, pages 51–70. 2010. ISBN 978-0-8243-5001-7. doi:10.1146/annurev-conmatphys-070909-104117.

[3] H Shishido, R Settai, H Harima, and Y Onuki. A drastic change of the fermi surface at a critical pressure in $CeRhIn_5$: dHvA study under pressure. *Journal of the Physical Society of Japan*, 74(4):1103–1106, Apr 2005. ISSN 0031-9015. doi:10.1143/JPSJ.74.1103.

[4] Philipp Gegenwart, Qimiao Si, and Frank Steglich. Quantum criticality in heavy-fermion metals. *Nature Physics*, 4(3):186–197, Mar 2008. ISSN 1745-2473. doi:10.1038/nphys892.

[5] P. Walmsley, C. Putzke, L. Malone, I. Guillamon, D. Vignolles, C. Proust, S. Badoux, A. I. Coldea, M. D. Watson, S. Kasahara, Y. Mizukami, T. Shibauchi, Y. Matsuda, and A. Carrington. Quasiparticle Mass Enhancement Close to the Quantum Critical Point in $BaFe_2(As_{1-x}P_x)_2$. *Physical Review Letters*, 110(25), Jun 21 2013. ISSN 0031-9007. doi: 10.1103/PhysRevLett.110.257002.

[6] A Liam Fitzpatrick, Shamit Kachru, Jared Kaplan, Steven A Kivelson, and S Raghu. Slow fermions in quantum critical metals. *arXiv preprint arXiv:1402.5413*, 2014.

[7] P. Monthoux, D. Pines, and G. G. Lonzarich. Superconductivity without phonons. *Nature*, 450(7173):1177–1183, Dec 20 2007. ISSN 0028-0836. doi:10.1038/nature06480.

[8] PW Anderson, PA Lee, M Randeria, TM Rice, N Trivedi, and FC Zhang. The physics behind high-temperature superconducting cuprates: the 'plain vanilla' version of rvb. *Journal of Physics-Condensed Matter*, 16(24):R755–R769, Jun 23 2004. ISSN 0953-8984. doi: 10.1088/0953-8984/16/24/R02.

[9] JL Tallon and JW Loram. The doping dependence of T^* - what is the real $high - T_c$ phase diagram? *Physica C*, 349(1-2):53–68, Jan 1 2001. ISSN 0921-4534. doi:10.1016/S0921-

4534(00)01524-0.

[10] G Grissonnanche, O Cyr-Choiniere, F Laliberte, S Rene de Cotret, A Juneau-Fecteau, S Dufour-Beausejour, M-E Delage, D LeBoeuf, J Chang, B.J. Ramshaw, D. A. Bonn, W. N. Hardy, Ruixing Liang, S. Adachi, N. E. Hussey, B. Vignolle, C. Proust, M. Sutherland, S. Kramer, J.-H. Park, D. Graf, N. Doiron-Leyraud, and Louis. Taillefer. Direct measurement of the upper critical field in a cuprate superconductor. *Nature Communications*, 5, Feb 2014. doi:/10.1038/ncomms4280.

[11] Jing Xia, Elizabeth Schemm, G. Deutscher, S. A. Kivelson, D. A. Bonn, W. N. Hardy, R. Liang, W. Siemons, G. Koster, M. M. Fejer, and A. Kapitulnik. Polar Kerr-effect measurements of the high-temperature $YBa_2Cu_3O_{6+x}$ superconductor: Evidence for broken symmetry near the pseudogap temperature. *Physical Review Letters*, 100(12), Mar 28 2008. ISSN 0031-9007. doi:10.1103/PhysRevLett.100.127002.

[12] Yuan Li, V Balédent, Neven Barišić, YC Cho, Y Sidis, G Yu, X Zhao, P Bourges, and M Greven. Magnetic order in the pseudogap phase of hgba 2 cuo 4+ δ studied by spin-polarized neutron diffraction. *Physical Review B*, 84(22):224508, 2011.

[13] A. Shekhter, B. J. Ramshaw, R. D. McDonald, J. B. Betts, F. Balakirev, Ruixing Liang, W. N. Hardy, D. A. Bonn, Scott C. Riggs, and Albert Migliori. Bounding the pseudogap with a line of phase transitions in $YBa_2Cu_3O_{6+\delta}$. *Nature*, 498(7452):75–77, 2013.

[14] S Blanco-Canosa, A Frano, E Schierle, J Porras, T Loew, M Minola, M Bluschke, E Weschke, B Keimer, and M Le Tacon. Resonant x-ray scattering study of charge density wave correlations in yba _2 cu _3 o _{6 + x}. *arXiv preprint arXiv:1406.1595*, 2014.

[15] K Fujita, Chung Koo Kim, Inhee Lee, Jinho Lee, MH Hamidian, IA Firmo, S Mukhopadhyay, H Eisaki, S Uchida, MJ Lawler, E.-A. Kim, and J.C. Davis. Simultaneous transitions in cuprate momentum-space topology and electronic symmetry breaking. *arXiv preprint arXiv:1403.7788*, 2014.

[16] CM Varma. Pseudogap phase and the quantum-critical point in copper-oxide metals. *Physical Review Letters*, 83(17):3538–3541, OCT 25 1999. ISSN 0031-9007. doi: 10.1103/PhysRevLett.83.3538.

[17] S Chakravarty, RB Laughlin, DK Morr, and C Nayak. Hidden order in the cuprates. *Physical Review B*, 63(9), MAR 1 2001. ISSN 0163-1829. doi:10.1103/PhysRevB.63.094503.

[18] Subir Sachdev. *Quantum phase transitions*. Wiley Online Library, 2007.

[19] Patrick A. Lee. From high temperature superconductivity to quantum spin liquid: progress in strong correlation physics. *Reports on Progress in Physics*, 71(1), Jan 2008. ISSN 0034-4885. doi:10.1088/0034-4885/71/1/012501.

[20] SA Kivelson, E Fradkin, and VJ Emery. Electronic liquid-crystal phases of a doped Mott insulator. *Nature*, 393(6685):550–553, Jun 11 1998. ISSN 0028-0836.

[21] R. Daou, J. Chang, David LeBoeuf, Olivier Cyr-Choinière, Francis Laliberte, Nicolas Doiron-Leyraud, B. J. Ramshaw, Ruixing Liang, D. A. Bonn, W. N. Hardy, and Louis Taillefer. Broken rotational symmetry in the pseudogap phase of a high-T_c superconductor. *Nature*, 463(7280):519–522, Jan 28 2010. ISSN 0028-0836. doi:10.1038/nature08716.

[22] B. J. Ramshaw, Baptiste Vignolle, James Day, Ruixing Liang, W. N. Hardy, Cyril Proust, and D. A. Bonn. Angle dependence of quantum oscillations in $YBa_2Cu_3O_{6.59}$ shows free-spin behaviour of quasiparticles. *Nature Physics*, 7(3):234–238, Mar 2011. ISSN 1745-2473. doi:10.1038/NPHYS1873. URL `http://dx.doi.org/10.1038/nphys1873`.

[23] Tao Wu, Hadrien Mayaffre, Steffen Krämer, Mladen Horvatić, Claude Berthier, Philip L Kuhns, Arneil P Reyes, Ruixing Liang, WN Hardy, DA Bonn, et al. Emergence of charge order from the vortex state of a high-temperature superconductor. *Nature communications*, 4, 2013.

[24] G. Ghiringhelli, M. Le Tacon, M. Minola, S. Blanco-Canosa, C. Mazzoli, N. B. Brookes, G. M. De Luca, A. Frano, D. G. Hawthorn, F. He, T. Loew, M. Moretti Sala, D. C. Peets, M. Salluzzo, E. Schierle, R. Sutarto, G. A. Sawatzky, E. Weschke, B. Keimer, and L. Braicovich. Long-range incommensurate charge fluctuations in (y,nd)ba2cu3o6+x. *SCIENCE*, 337(6096):821–825, AUG 17 2012. ISSN 0036-8075. doi:10.1126/science.1223532.

[25] J. Chang, A. T. Blackburn, N. B. Holmes, J. Christensen, J. Larsen, J. Mesot, Ruixing Liang, D. A. Bonn, W. N. Hardy, A. Watenphul, M. v. Zimmerman, E. M. Forgan, and S. M. Hayden. Direct observation of competition between superconductivity and charge density wave order in $YBa_2Cu_3O_y$. *Nature Physics*, Oct 2012. doi:10.1038/nphys2456. URL `http://dx.doi.org/10.1038/nphys2456`.

[26] M Huecker, NB Christensen, AT Holmes, E Blackburn, EM Forgan, Ruixing Liang, DA Bonn, WN Hardy, O Gutowski, M v Zimmermann, et al. Competing charge, spin, and superconducting orders in underdoped yba2cu3oy. *arXiv preprint arXiv:1405.7001*, 2014.

[27] R. Comin, A. Frano, M. M. Yee, Y. Yoshida, H. Eisaki, E. Schierle, E. Weschke, R. Sutarto,

F. He, A. Soumyanarayanan, Yang He, M. Le Tacon, I. S. Elfimov, Jennifer E. Hoffman, G. A. Sawatzky, B. Keimer, and A. Damascelli. Charge order driven by fermi-arc instability in bi2sr2-xlaxcuo6+delta. *Science*, 343(6169):390–392, JAN 24 2014. ISSN 0036-8075. doi: 10.1126/science.1242996.

[28] D. Shoenberg. *Magnetic oscillations in metals*. Cambridge monographs on physics. Cambridge University Press, 1984. ISBN 9780521224802.

[29] Nicolas Doiron-Leyraud, Cyril Proust, David LeBoeuf, Julien Levallois, Jean-Baptiste Bonnemaison, Ruixing Liang, D. A. Bonn, W. N. Hardy, and Louis Taillefer. Quantum Oscillations and the Fermi Surface in an Underdoped High-T_c Superconductor. *Nature*, 447(7144):565–568, May 31 2007. ISSN 0028-0836. doi:10.1038/nature05872.

[30] David LeBoeuf, Nicolas Doiron-Leyraud, Julien Levallois, R. Daou, J.-B. Bonnemaison, N. E. Hussey, L. Balicas, B. J. Ramshaw, Ruixing Liang, D. A. Bonn, W. N. Hardy, S. Adachi, Cyril Proust, and Louis Taillefer. Electron pockets in the fermi surface of hole-doped high-t-c superconductors. *Nature*, 450(7169):533–536, Nov 22 2007. ISSN 0028-0836. doi: 10.1038/nature06332.

[31] E. A. Yelland, J. Singleton, C. H. Mielke, N. Harrison, F. F. Balakirev, B. Dabrowski, and J. R. Cooper. Quantum oscillations in the underdoped cuprate $yba_2cu_4o_8$. *Phys. Rev. Lett.*, 100:047003, Feb 2008. doi:10.1103/PhysRevLett.100.047003. URL `http://link.aps.org/doi/10.1103/PhysRevLett.100.047003`.

[32] A. F. Bangura, J. D. Fletcher, A. Carrington, J. Levallois, M. Nardone, B. Vignolle, P. J. Heard, N. Doiron-Leyraud, D. LeBoeuf, L. Taillefer, S. Adachi, C. Proust, and N. E. Hussey. Small fermi surface pockets in underdoped high temperature superconductors: Observation of shubnikov-de haas oscillations in yba(2)cu(4)o(8). *Physical Review Letters*, 100(4), FEB 1 2008. ISSN 0031-9007. doi:10.1103/PhysRevLett.100.047004.

[33] Neven Barišić, Sven Badoux, Mun K Chan, Chelsey Dorow, Wojciech Tabis, Baptiste Vignolle, Guichuan Yu, Jérôme Béard, Xudong Zhao, Cyril Proust, and Martin Greven. Universal quantum oscillations in the underdoped cuprate superconductors. *Nature Physics*, 9(12):761–764, 2013.

[34] Baptiste Vignolle, David Vignolles, David LeBoeuf, Stephane Lepault, Brad Ramshaw, Ruixing Liang, D. A. Bonn, W. N. Hardy, Nicolas Doiron-Leyraud, A. Carrington, N. E. Hussey, Louis Taillefer, and Cyril Proust. Quantum oscillations and the Fermi surface of high-

temperature cuprate superconductors. *Comptes Rendus Physique*, 12(5-6):446–460, Jun-Aug 2011. ISSN 1631-0705. doi:10.1016/j.crhy.2011.04.011.

[35] Suchitra E. Sebastian, N. Harrison, M. M. Altarawneh, Ruixing Liang, D. A. Bonn, W. N. Hardy, and G. G. Lonzarich. Fermi-liquid behavior in an underdoped high-T_c superconductor. *Phys. Rev. B*, 81:140505, Apr 2010. doi:10.1103/PhysRevB.81.140505. URL `http://link.aps.org/doi/10.1103/PhysRevB.81.140505`.

[36] Z-X Shen, A Lanzara, S Ishihara, and N Nagaosa. Role of the electron-phonon interaction in the strongly correlated cuprate superconductors. *Philosophical Magazine B*, 82(13):1349–1368, 2002.

[37] Rikio Settai, Tetsuya Takeuchi, and Yoshichika Ōnuki. Recent advances in ce-based heavy-fermion superconductivity and fermi surface properties. *Journal of the Physical Society of Japan*, 76(5), 2007.

[38] M. Huecker, M. v. Zimmermann, G. D. Gu, Z. J. Xu, J. S. Wen, Guangyong Xu, H. J. Kang, A. Zheludev, and J. M. Tranquada. Stripe order in superconducting $La_{2-x}Ba_xCuO_4$ (0.095 <= x <= 0.155). *Physical Review B*, 83(10), Mar 17 2011. ISSN 1098-0121. doi: 10.1103/PhysRevB.83.104506.

[39] Suchitra E. Sebastian, N. Harrison, M. M. Altarawneh, C. H. Mielke, Ruixing Liang, D. A. Bonn, W. N. Hardy, and G. G. Lonzarich. Metal-insulator quantum critical point beneath the high T_c superconducting dome. *Proceedings of the National Academy of Sciences of the United States of America*, 107(14):6175–6179, Apr 6 2010. ISSN 0027-8424.

[40] HQ Yuan, FM Grosche, M Deppe, C Geibel, G Sparn, and F Steglich. Observation of two distinct superconducting phases in $CeCu_2Si_2$. *Science*, 302(5653):2104–2107, Dec 19 2003. ISSN 0036-8075. doi:10.1126/science.1091648.

[41] M. Le Tacon, G. Ghiringhelli, J. Chaloupka, M. Moretti Sala, V. Hinkov, M. W. Haverkort, M. Minola, M. Bakr, K. J. Zhou, S. Blanco-Canosa, C. Monney, Y. T. Song, G. L. Sun, C. T. Lin, G. M. De Luca, M. Salluzzo, G. Khaliullin, T. Schmitt, L. Braicovich, and B. Keimer. Intense paramagnon excitations in a large family of high-temperature superconductors. *Nature PhysicS*, 7(9):725–730, SEP 2011. ISSN 1745-2473. doi:10.1038/NPHYS2041.

[42] David LeBoeuf, Nicolas Doiron-Leyraud, B. Vignolle, Mike Sutherland, B. J. Ramshaw, J. Levallois, R. Daou, Francis Laliberté, Olivier Cyr-Choinière, Johan Chang, Y. J. Jo, L. Balicas, Ruixing Liang, D. A. Bonn, W. N. Hardy, Cyril Proust, and Louis Taillefer.

Lifshitz critical point in the cuprate superconductor yba$_2$cu$_3$o$_y$ from high-field hall effect measurements. *Phys. Rev. B*, 83:054506, Feb 2011. doi:10.1103/PhysRevB.83.054506. URL http://link.aps.org/doi/10.1103/PhysRevB.83.054506.

[43] David LeBoeuf, S. Kraemer, W. N. Hardy, Ruixing Liang, D. A. Bonn, and Cyril Proust. Thermodynamic phase diagram of static charge order in underdoped yba2cu3oy. *Nature Physics*, 9(2):79–83, Feb 2013. ISSN 1745-2473.

[44] Ruixing Liang, D. A. Bonn, and W. N. Hardy. Evaluation of CuO_2 plane hole doping in $YBa_2Cu_3O_{6+x}$ single crystals. *Phys. Rev. B*, 73:180505, May 2006. doi: 10.1103/PhysRevB.73.180505. URL http://link.aps.org/doi/10.1103/PhysRevB.73.180505.

[45] F. Coneri, S. Sanna, K. Zheng, J. Lord, and R. De Renzi. Magnetic states of lightly hole-doped cuprates in the clean limit as seen via zero-field muon spin spectroscopy. *Phys. Rev. B*, 81: 104507, Mar 2010. doi:10.1103/PhysRevB.81.104507. URL http://link.aps.org/doi/10.1103/PhysRevB.81.104507.

[46] John Singleton, Clarina de la Cruz, R. D. McDonald, Shiliang Li, Moaz Altarawneh, Paul Goddard, Isabel Franke, Dwight Rickel, C. H. Mielke, Xin Yao, and Pengcheng Dai. Magnetic Quantum Oscillations in $YBa_2Cu_3O_{6.61}$ and $YBa_2Cu_3O_{6.69}$ in Fields of Up to 85 T: Patching the Hole in the Roof of the Superconducting Dome. *Phys. Rev. Lett.*, 104:086403, Feb 2010. doi: 10.1103/PhysRevLett.104.086403. URL http://link.aps.org/doi/10.1103/PhysRevLett.104.086403.

[47] Y Ando, S Komiya, K Segawa, S Ono, and Y Kurita. Electronic phase diagram of high-T_c cuprate superconductors from a mapping of the in-plane resistivity curvature. *Physical Review Letters*, 93(26), Dec 31 2004. ISSN 0031-9007. doi:10.1103/PhysRevLett.93.267001.

[48] Suchitra E. Sebastian, Neil Harrison, and Gilbert G. Lonzarich. Towards resolution of the Fermi surface in underdoped high-T_c superconductors. *Reports on Progress in Physics*, 75 (10), Oct 2012. ISSN 0034-4885. doi:10.1088/0034-4885/75/10/102501.

[49] B. J. Ramshaw, James Day, Baptiste Vignolle, David LeBoeuf, P. Dosanjh, Cyril Proust, Louis Taillefer, Ruixing Liang, W. N. Hardy, and D. A. Bonn. Vortex lattice melting and H_{c2} in underdoped $YBa_2Cu_3O_y$. *Phys. Rev. B*, 86:174501, Nov 2012. doi:10.1103/PhysRevB.86.174501. URL http://link.aps.org/doi/10.1103/PhysRevB.86.174501.

[50] M Von Zimmermann, JR Schneider, T Frello, NH Andersen, J Madsen, M Kall, HF Poulsen,

R Liang, P Dosanjh, and WN Hardy. Oxygen-ordering superstructures in underdoped $YBa_2Cu_3O_{6+x}$ studied by hard x-ray diffraction. *Physical Review B*, 68(10):104515, Sep 1 2003. ISSN 1098-0121. doi:10.1103/PhysRevB.68.104515. URL `http://link.aps.org/doi/10.1103/PhysRevB.85.104515`.

I. ACKNOWLEDGEMENTS

This work is supported by the US Department of Energy BES "Science at 100 T," the National Science Foundation, the State of Florida, the Natural Science and Engineering Research Council of Canada and the Canadian Institute for Advanced Research. S.E.S. acknowledges support from the Royal Society and the European Research Council under the European Union's Seventh Framework Programme (FP7/2007-2013) / ERC Grant Agreement no. 337425. The authors gratefully acknowledge discussions with S. Chakravarty, S. Kivelson, M. Le Tacon, K.A. Modic, C. Proust, A. Shekhter, and L. Taillefer. We are indebted to J. Baglo for sharing his results on the effect of quenched oxygen disorder on the microwave scattering rate in $YBa_2Cu_3O_{6+\delta}$: without this advance, oscillations would not have been observed. Finally, we would like to acknowledge the entire 100 T operations team at the pulsed field facility for their support during the experiment. B.J.R., S.E.S., R.D.M., B.T., Z.Z., and N.H. performed the high-field resistivity measurements at the National High Magnetic Field Laboratory-Pulsed Field Facility. B.J.R., J.D., R.L., D.A.B., and W.N.H. grew and prepared the samples at the University of British Columbia. B.J.R. analysed the data. B.J.R wrote the manuscript, with contributions from S.E.S., R.D.M., N.H., J.D, D.A.B., and W.N.H.

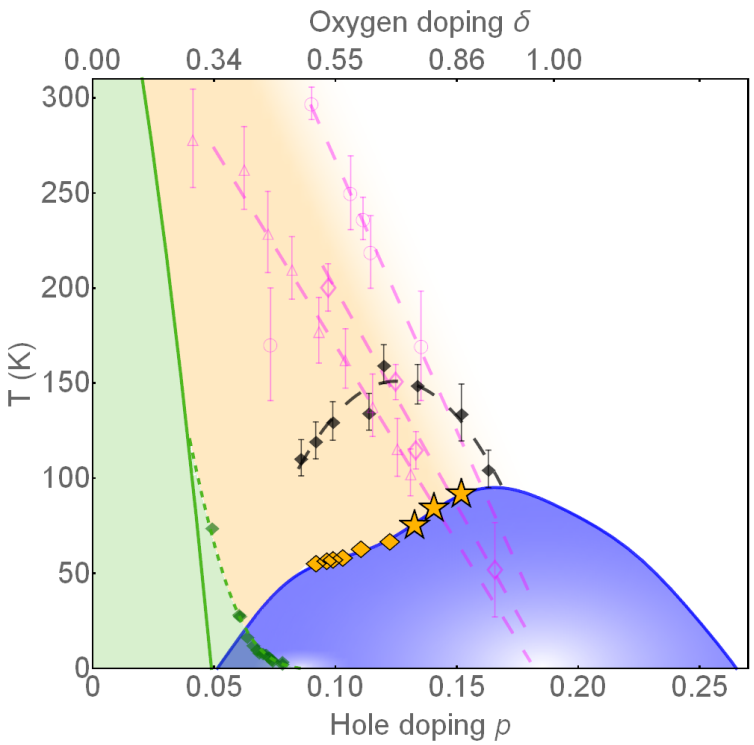

FIG. 1. **Fig. 1: High-T_c temperature-doping phase diagram.** Superconductivity is in blue(44), the antiferromagnetic (AFM) phase is in green (45), and the pseudogap is in orange. Orange diamonds designate dopings where quantum oscillations have been observed previously(34, 46), and stars denote the new dopings presented in this paper. Short-range antiferromagnetic order (green diamonds) terminates at a quantum critical point at $p = 0.08$ (39); beyond $p = 0.08$, short-range charge order onsets above T_c (black diamonds)(14, 26). The charge order, the onset of the pseudogap (as defined by neutron spin-flip scattering (pink circles)(12), the polar Kerr effect (pink diamonds)(11), and the change in the slope of resistivity with temperature (pink triangles)(47)) terminate near $p = 0.18$, suggesting the possibility of a quantum critical point at this doping.

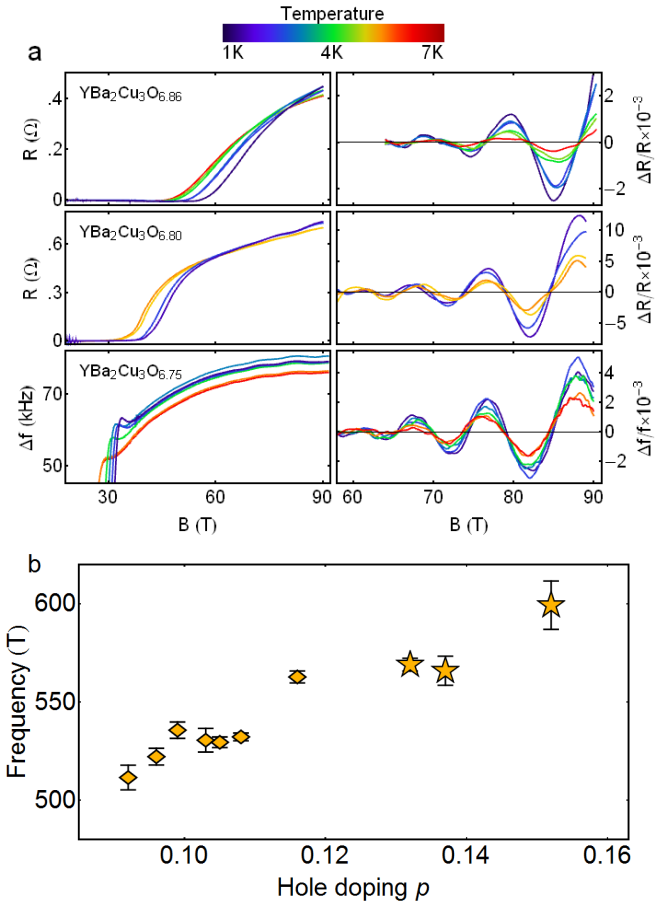

FIG. 2. **Fig. 2: Quantum oscillations of the magnetoresistance.** The bare (left panels) and oscillatory component (right panels) of the magnetoresistance (**a**). $\hat{c}$-axis transport was measured for $\delta = 0.80$ and 86; skin depth, measured via frequency shift of an oscillatory circuit (see S.I.), was measured for $\delta = 0.75$. A smooth, non-oscillatory background is removed from the data to extract the oscillatory component (see S.I. for details of the analysis). The quantum oscillation amplitude is suppressed by a factor of two between 1.5 and 6 K in $YBa_2Cu_3O_{6.75}$, compared to a factor of five over the same temperature range in $YBa_2Cu_3O_{6.86}$, indicating an increased effective mass for the higher doped sample. Quantum oscillation frequency, proportional to Fermi-surface area, as a function of hole doping (**b**), with dopings below $p = 0.12$ taken from Sebastian et al. (48). The frequencies and their uncertainties were obtained as described in the methods.

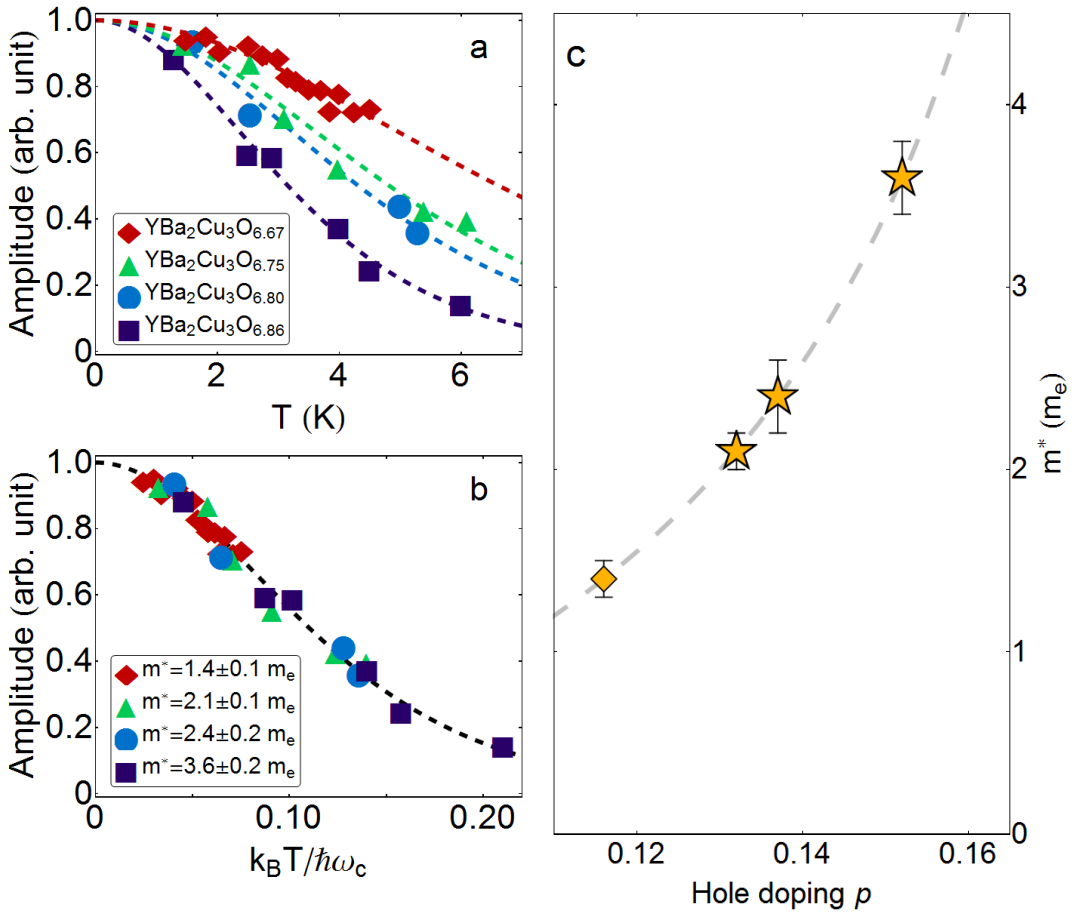

FIG. 3. **Fig. 3: The quasiparticle effective mass.** Quantum oscillation amplitude as a function of temperature, (**a**), and as a function of the ratio of thermal to cyclotron energy $k_BT/\hbar\omega_c$, (**b**). Also included is detailed temperature dependence of $YBa_2Cu_3O_{6.67}$—a composition at which oscillations have previously been reported(46). Panel **a** illustrates the increase in $m^\star$ with increased hole doping, with fits to Equation 1. Panel **b** shows the same data versus $k_BT/\hbar\omega_c^\star$, where $\omega_c^\star = eB/m^\star$: this scaling with $m^\star$ shows the robustness of the fit across the entire doping and temperature range. The effective mass as a function of hole doping is plotted in **c**—error bars are the standard error from regression of Equation 1 to the data. The dashed line is a guide to the eye.

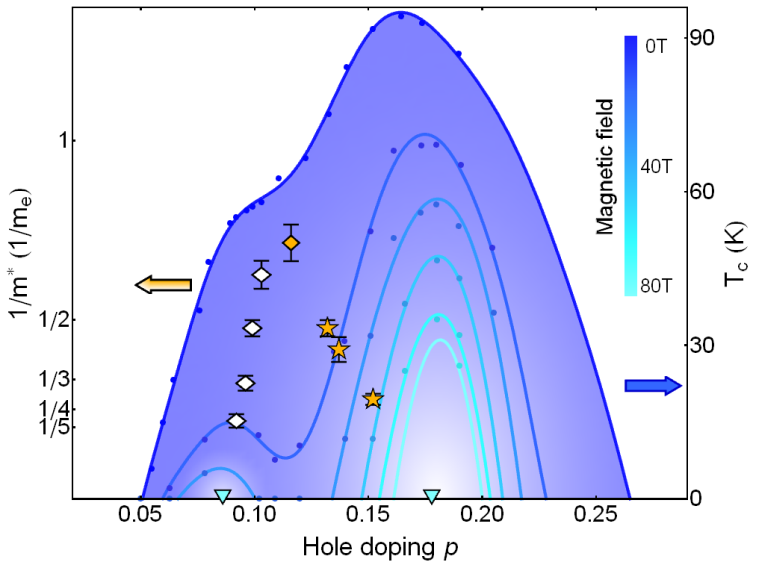

FIG. 4. **Fig. 4: A quantum critical point near optimal doping.** The blue curves correspond to T_c, as defined by the resistive transition (right axis), at magnetic fields of 0, 15, 30, 50, 70, and 82 T (data points taken from Grissonnanche et al. (10), Ramshaw et al. (49), and unpublished data on $YBa_2Cu_3O_{6.998}$ at 82 T). As the magnetic field is increased, the superconducting T_c is suppressed. By 30 T two separate domes remain, centred around $p \approx 0.08$ and $p \approx 0.18$; by 82 T only the dome at $p \approx 0.18$ remains. The inverse of the effective mass has been overlaid on this phase diagram (left axis), extrapolating to maximum mass enhancement at at $p \approx 0.08$ and $p \approx 0.18$ (white points taken from Sebastian et al. (48)). This makes explicit the connection between effective mass enhancement and the strength of superconductivity, which both converge on QCPs (marked by cyan triangles).

II. MATERIALS AND METHODS

Samples: $YBa_2Cu_3O_{6+\delta}$ samples were prepared for transport measurements in the same manner as in our previous studies.(22, 29) Prior to measurement, samples were heated above the ortho-III and ortho-VIII phase transition temperatures(50) to disorder the oxygen in the chains, and then quenched in liquid nitrogen. This process changes the nature of the oxygen defects in $YBa_2Cu_3O_{6+\delta}$, and enables the observation of quantum oscillations by increasing the quasiparticle lifetime.

Measurement: Four-point $\hat{c}$-axis electrical resistance was measured for $YBa_2Cu_3O_{6.80}$ and $YBa_2Cu_3O_{6.86}$ using a digital lock-in amplifier. Skin-depth, proportional to $\hat{a}-\hat{b}$–plane resistance, was measured using a proximity diode oscillator on $YBa_2Cu_3O_{6.67}$ and $YBa_2Cu_3O_{6.75}$.(39) All pulsed field measurements—up to 92 T for $YBa_2Cu_3O_{6.86}$, $YBa_2Cu_3O_{6.80}$, and $YBa_2Cu_3O_{6.75}$; up to 65 T for $YBa_2Cu_3O_{6.67}$—were made at the National High Magnetic Field Laboratory–Pulsed Field Facility.

Analysis: The temperature-dependent amplitude $A(T)$ is extracted from the oscillatory magnetoresistance by fitting the standard Lifshitz-Kosevich expression for a quasi-2D Fermi surface(22) $\frac{\Delta R}{R} = A(T)\, e^{-\frac{\pi}{\omega_c \tau}} \cos\left(\frac{2\pi F}{B}\right) J_0\left(\frac{2\pi \Delta F}{B}\right)$ at each temperature, keeping τ, F, and ΔF fixed for a particular doping. The mass is then obtained by fitting the amplitude $A(T)$ to Equation 1. More details of the data analysis, including the procedure for background removal, can be found in the S.I.

Because of the small number of oscillations available at high doping, the frequency F was obtained in three different ways to check for consistency: by fitting the oscillatory component to the Lifshitz-Kosevich expression above; by Fourier-transforming the oscillatory data; and by Landau-indexing the oscillation peak positions.(34) The uncertainties in F shown in Figure 2b were obtained from the Fourier transform peak widths. While there are systematic differences of about 3% between the three methods of frequency determination, the trend of F with hole doping p is the same to within the uncertainty.